Published in final edited form as:
J Neurosurg Pediatr. 2014 March ; 13(3): 276–282. doi:10.3171/2013.11.PEDS136.

Magnetic resonance imaging properties of convective delivery in diffuse intrinsic pontine gliomas

Prashant Chittiboina, M.D., M.P.H.[1], **John D. Heiss, M.D.**[1], **Katherine E. Warren, M.D.**[2], and **Russell R. Lonser, M.D.**[1,3]

[1]Surgical Neurology Branch, National Institute of Neurological Disorders and Stroke, Bethesda, Maryland [2]Pediatric Oncology Branch, Center for Cancer Research, National Cancer Institute, Bethesda, Maryland [3]Department of Neurological Surgery, The Ohio State University Wexner Medical Center, Columbus, Ohio

Abstract

Object—Coinfused surrogate imaging tracers can provide direct insight into the properties of convection-enhanced delivery (CED) in the nervous system. To better understand the distributive properties of CED in a clinical circumstance, the authors analyzed the imaging findings in pediatric diffuse intrinsic pontine glioma (DIPG) patients undergoing coinfusion of Gd-DTPA and interleukin-13–*Pseudomonas* exotoxin (IL13-PE).

Methods—Consecutive patients undergoing CED (maximal rates of 5 or 10 μl/minute) of Gd-DTPA (1 or 5 mM) and IL13-PE (0.125 μg/ml or 0.25 μg/ml) for DIPG were included. Real-time MRI was performed during infusions, and imaging results were analyzed.

Results—Four patients (2 males, 2 females; mean age at initial infusion 13.0 ± 5.3 years; range 5–17 years) underwent 5 infusions into DIPGs. Brainstem infusions were clearly identified on T1-weighted MR images at 1-mM (1 infusion) and 5-mM (4 infusions) coinfused Gd-DTPA concentrations. While the volume of distribution (Vd) increased progressively with volume of infusion (Vi) (mean volume 2.5 ± 0.9 ml; range 1.1–3.7 ml), final Vd:Vi ratios were significantly reduced with lower Gd-DTPA concentration (Vd:Vi for 1 mM of 1.6 compared with a mean Vd:Vi ratio for 5 mM of 3.3 ± 1.0) ($p = 0.04$). Similarly, anatomical distribution patterns were affected by preferential flow along parallel axial fiber tracts, into prior infusion cannula tracts and intraparenchymal air pockets, and leak back around the infusion cannula at the highest rate of infusion.

Address correspondence to: Russell R. Lonser, M.D., Department of Neurological Surgery, The Ohio State University Wexner Medical Center, Doan Hall, Rm. 1047, Columbus, OH 43210. russell.lonser@osumc.edu.

Author contributions to the study and manuscript preparation include the following. Conception and design: Lonser. Acquisition of data: Chittiboina, Heiss, Warren. Analysis and interpretation of data: Lonser, Chittiboina, Warren. Drafting the article: Chittiboina. Critically revising the article: all authors. Reviewed submitted version of manuscript: all authors. Approved the final version of the manuscript on behalf of all authors: Lonser. Study supervision: Lonser, Warren.

Disclosure
Dr. Lonser holds a patent with NIH.

Conclusions—Magnetic resonance imaging of a coinfused Gd-DTPA surrogate tracer provided direct insight into the properties of CED in a clinical application. While clinically relevant Vds can be achieved by convective delivery, specific tissue properties can affect distribution volume and pattern, including Gd-DTPA concentration, preferential flow patterns, and infusion rate. Understanding of these properties of CED can enhance its clinical application. Part of clinical trial no. NCT00880061 (ClinicalTrials.gov).

Keywords

convection-enhanced delivery; brainstem glioma; imaging; gadolinium; magnetic resonance imaging; oncology

---

While the properties of convective delivery have been defined in naïve nervous system tissue of small and large animal models,[3,4,10,11,18,19,21,27,33] the properties of convection-enhanced delivery (CED) under the pathological conditions encountered in human clinical applications are not understood. Insight into convective properties in clinical circumstances will be critical to successfully applying convective drug delivery to the treatment of currently untreatable neurological disorders and to developing predictive modeling paradigms. The application of coinfused MRI surrogate tracers now provides an opportunity to gain direct and potent insights into the clinical use of convective drug distribution in real time in a noninvasive manner.

Preclinical data indicate that Gd-DTPA can be used in MRI to accurately monitor convective drug delivery over a wide range of clinical applications and putative therapeutic compounds. Specifically, autoradiographic analysis demonstrates that Gd-DTPA can accurately track large-molecular-weight compounds, including proteins, over the volume of infusion (Vi) necessary to treat brainstem disorders. [1,5,15,26] To develop deeper understanding i nto CED properties, we coinfused Gd-DTPA with interleukin-13 bound to *Pseudomonas* exotoxin (IL13-PE; MW 52 kD) into diffuse intrinsic pontine gliomas (DIPGs). Imaging findings were analyzed to determine factors that affect volume of distribution (Vd) and anatomical distribution pattern of the infusate in tumor-infiltrated tissues.

Methods

Patients

We included 4 consecutive pediatric patients enrolled in a Phase I study in which the glioma toxin IL13-PE was coinfused with Gd-DTPA (NIH no. 09-N-0117) to treat DIPGs. Informed consent was obtained from the legal guardians of these minor patients. This study is part of a larger clinical trial (NCT00880061 at clinicaltrials.gov).

IL13-PE and Gd-DTPA Infusate

The toxin IL13-PE (InSys Therapeutics, Inc.) was thawed and diluted with 0.9% normal saline containing 0.2% human serum albumin.[12] The Gd-DTPA solution (469 mg/ml) (Magnevist, Bayer Healthcare Pharmaceuticals, Inc.) was combined with IL13-PE to

achieve a final Gd-DTPA concentration 1 or 5 mM in a final concentration of IL13-PE of either 0.125 or 0.25 μg/ml.

Infusion Technique

Frameless Stereotactic Surgical Approach—For the patients in Cases 1 and 2 (Table 1), a frameless stereotactic surgical technique was used with a Vygon catheter or Nex-Gen cannula. Briefly, the day before surgery, 3D volumetric MR images were obtained for the surgical navigation (StealthStation, Medtronic, Inc.) to place the infusion catheter/cannula. On the day of surgery, general anesthesia was induced, and the patient's head was registered in the surgical navigation system. After preparation and incision, a bur hole was placed and the dura opened. The catheter/cannula was inserted using stereotactic navigation guidance. The Vygon catheter (2-mm outer diameter and 1-mm inner diameter [Case 1]) was tunneled posterolaterally and secured by a nylon suture and the wound was closed. The NexGen inner infusion cannula was secured within the outer cannula guide (Case 2), and the scalp was closed around the cannula. The final position of the catheter or inner infusion cannula was confirmed with intraoperative MRI (Achieva 1.5-T, Philips). The infusion catheter/cannula was coupled to the infusion tubing, and the infusion was started.

MRI-Guided Stereotactic Approach—In the patients in Cases 3 and 4 (Table 1), MRI-guided stereotactic CED procedures were performed with the SmartFlow cannula and ClearPoint system (MRI Interventions, Inc.).[23] Briefly, after induction of general anesthesia and positioning of the patient, the patient's head was fixed with an MRI-compatible head clamp (Integra LifeSciences Corp.), and imaging surface coils were placed around the head. A scan was obtained after placing a localizing grid (MRI Interventions, Inc.) over the ipsilateral frontal region. The surgical trajectory was planned, the incision site prepared, and incision made. A bur hole was placed and the dura opened. The ClearPoint aiming device was used to advance the cannula to its final position. Before starting the infusion, a MR image was acquired to confirm the trajectory and final position of the cannula tip. The infusion cannula was connected to the pump and infusion started.

Infusate Delivery—Convective delivery of Gd-DTPA and IL13-PE was performed using a Medfusion Model 3500 (Smiths Medical) syringe infusion pump.[18] Starting at 0.5 ml/minute, the infusion rate was increased by 0.5 μl/minute every 10 minutes until maximal rate was achieved (Table 1).

Intraoperative MRI—Magnetic resonance imaging was performed throughout the infusions.[18] Axial FLAIR images were used to assess infusate leakage into the CSF during infusion.[10,18]

Imaging Analysis

OsiriX software (Pixmeo) was used to calculate tissue Vd based on MRI. This software uses the Insight Segmentation and Registration Toolkit (ITK) developed at the National Institutes of Health.[24] A connected thresholding technique for growing a region of interest (ROI) was used to determine Vd.[29] T1-weighted sequences were used for calculating Vd by placing a seed voxel within the infused region near the catheter tip and growing the region of infusion

based on a specified threshold. Specifically, the seed voxel was placed after identifying the local maximum intensity voxels, and the ROI was grown to include the entire contrast-enhancing region by modulating the interval threshold. This allowed the inclusion of only the neighboring voxels whose intensity value was within the specified threshold. Once a 3D ROI was created, a Vd for the infusion was obtained.

Statistical Analysis

The 1-sided unpaired Student t-test was used to compare final Vd:Vi ratios. Statistical significance was achieved if a p value was less than 0.05.

Results

Patient Characteristics

Four pediatric patients (2 males, 2 females; mean age at initial infusion 13.0 ± 5.3 years, range 5–17 years) underwent 5 infusions into DIPGs (Table 1).

Infusion Characteristics

We acquired T1-weighted MR images within 2 minutes of starting infusions. A feature of successful infusion initiation was the presence of clearly visible infusate at the cannula tip within 2 minutes of starting the infusion. Ninety-five minutes into the infusion in Case 3 (first infusion; Table 1), MRI showed that the infusate failed to continue progress. Inspection of the pump and infusion tubing revealed leakage of the infusate at the distal end of the inline filter connection. The connector was replaced and infusion restarted without further leakage. Real-time imaging revealed progressive increase in Vd for the duration of infusion.

Factors Affecting Vd

Concentration Contrast Material—Contrast from both concentrations of the Gd-DTPA surrogate tracer (1 mM and 5 mM) could be clearly identified during infusion on T1-weighted MRI within the perfused region (Table 1). Whereas the patient in Case 1 underwent infusion of 1 mM Gd-DTPA during infusion of IL13-PE, the patients in Cases 2 through 4 underwent infusion of 5 mM Gd-DTPA during infusion of IL13-PE. The 1-mM Gd-DTPA concentration was associated with lower final Vd:Vi ratio of 1.6 compared with the 5-mM Gd-DTPA concentration (3.3 ± 1.0 [p = 0.04, 95% CI 0.1–3.2]).

Factors Affecting Distribution Pattern

Intraparenchymal Air at the Cannula Tip—In Case 1 an air pocket formed at the catheter tip after removal of the inner stylet and once infusion was initiated. The intraparenchymal air remained at the catheter tip site throughout the infusion and altered the distribution pattern. The anteromedial air pocket inhibited anteromedial spread of the infusate, which reduced the anterior and medial perfusion of the brainstem and tumor (Fig. 1).

Anatomical Fiber Tracts—Preferential infusate flow was identified in Cases 2, 3, and 4 along parallel white matter tracts oriented in the axial plane of the brainstem. During early

periods of the infusion in these patients, the infusate preferentially filled axially oriented fibers of the pons but spared the perpendicularly oriented fibers of the corticospinal tract. With infusion progression, the infusate entered the perpendicularly oriented corticospinal fiber tracts (Fig. 2).

Prior Cannula Tract—The patient in Case 3 underwent reinfusion 4 weeks after initial infusion (Table 1). The cannula tip was placed 23 mm posterior to the previous cannula tract. Once the leading edge of the second infusion encountered the prior cannula tract, the infusate preferentially flowed into and up through the initial cannula tract (Fig. 3). This led to preferential redirection of the infusate to regions of brain surrounding the previous cannula tract. The cannula was repositioned deeper into the tumor and reflux into prior cannula tract was ameliorated.

Leak Back Around Cannula—Leak back around the infusion cannula was identified in Case 4 at the highest rate of infusion (10 μl/minute). The infusate leak back resulted in an elongated configuration of drug distribution around and along the cannula (Fig. 4), as the infusate was distributed preferentially along the cannula during the infusion.

Discussion

Imaging of Convective Delivery

Previously, our understanding of the properties of convective delivery in the nervous system has been based on data derived from infusions into the nervous system of naïve and diseased animals.[2,4–8,10] While these data have been critical to understanding the properties of CED in nervous system tissues without disease, a direct understanding of convective properties in humans and in variable disease conditions is lacking. Recently, imaging surrogates for real-time monitoring of drug distribution have been validated in preclinical models as safe and accurate methods for tracking infusate delivery.[1,9,10,16,19,27,34] These findings permit the critical application of real-time imaging of convective delivery to various human disease conditions.

Previous Clinical Trials

Poor infusate distribution may lead to inaccurate estimation of the cytotoxic efficacy of an agent after CED for brain tumors.[12,13,25] Several advanced clinical trials have failed to show an advantage for CED of putative therapeutics in the preclinical setting and in early clinical trials. Because distribution of drug delivery was not assessed concurrently with infusion, the true effectiveness of these putative therapeutic agents is not known. Furthermore, the properties of convective delivery in clinical trials remain to be determined, as real-time monitoring of drug delivery has not been performed routinely in the clinical setting. We have described the imaging findings associated with coinfusion Gd-DTPA and IL13-PE in pediatric patients with DIPGs in whom distribution was shown in real time by MRI.

Current Study

The imaging findings from the current study provide early and important understanding of the application of CED to tumor-infiltrated tissues in humans. Based on the clearly defined

imaging characteristics of Gd-DTPA coinfusion with a putative therapeutic agent (IL13-PE), a number of features associated with CED in the clinical setting could be defined. Based on these findings, clinically relevant volumes of drug delivery can be achieved during an acute infusion. Furthermore, data obtained in these patients provide direct insight into the effects of infusion mechanics, tracer concentration, cannula design, anatomical pathways, prior cannula tracts, and infusion rate.

Mechanical Problems—Real-time MRI of a coinfused surrogate imaging tracer during convective infusion provides an opportunity to establish the mechanical effectiveness of infusions by monitoring perfusion progress. Within 2 minutes of initiating the infusion, contrast material could be seen at the tip of the infusion catheter/cannula, confirming patency and mechanical function of the infusion system in each case. During one infusion (Case 3, Infusion 1), the Vd failed to progress because the infusate leaked from the point where the infusion tubing connected with the distal end of the inline filter. The infusion was stopped and tubing and inline filter were replaced, which prevented further leakage. The infusion was restarted with expected increases in the Vd until IL13-PE perfusion was completed.

Concentration of Gd-DTPA—Recently, in preclinical nonhuman primate studies, Asthagiri and colleagues[1] demonstrated that the concentration of Gd-DTPA affects the imaging Vd and the accuracy of drug tracking. Specifically, a 1-mM concentration of Gd-DTPA (which was the concentration used in our Case 1) underestimates the Vd of coinfused low- and high-molecular-weight compounds. Alternatively, a concentration of 5 mM Gd-DTPA accurately tracked low- and high-molecular-weight compounds (12% and 0.2% difference between actual drug Vd and imaged Vd, respectively). Consistent with the previous findings, the current study demonstrated that MRI of a 1-mM Gd-DTPA distribution volume (mean Vd:Vi 1.6) was significantly less than the distribution volume of a 5-mM infusion (mean Vd:Vi 3.3).

Cannula Design—Features of cannula/catheter design significantly impact distribution of the infusate. Specifically, we used a soft, malleable catheter with an inner stylet (stylet used for catheter rigidity during placement) for infusion in Case 1. Air was entrained within the dead space of the catheter after the stylet was removed, was delivered into the parenchyma surrounding the catheter tip, and was clearly identified on MRI. During the course of infusion, contemporaneous MRI of the Gd-DTPA-containing infusate demonstrated that the intraparenchymal air reduced the anteromedial spread of the infusate into tumor in that region. Therefore, in subsequently treated patients, the infusion was performed with stylet-less rigid cannula filled with infusate before placement,[23] which eliminated this problem.

The effect of intraparenchymal air at the infusion site provides direct insight into potential drug distribution problems associated with prior clinical trials that used this or similarly designed catheters.[12,13] Specifically, it is likely that intraparenchymal air altered the infusate distribution pattern in the patients undergoing infusion in those trials. Because these trials did not monitor infusate distribution in real time, the impact of this feature cannot be quantified, but the effect of air in our patient was clearly demonstrated by the altered anatomical distribution of the infusate. These findings underscore the importance of imaging

during convective delivery and the use of a rigid infusion-delivery cannula that can be placed precisely in a targeted region and does not contain dead space air that can be delivered into the parenchyma.[23]

Anatomical Pathways—Previous studies in naïve animal have shown that the infusate distributes preferentially along parallel white matter tracts.[4,14,17,19,30,31] Consistent with these data, when infusion cannulas were placed in the pons, the infusate distributed uniformly and radially along axially oriented fibers until the leading edge of the infusion encountered the coronally oriented corticospinal tracts. At this point, the infusate continued to preferentially fill along the axial fibers but ultimately filled along the perpendicularly oriented corticospinal tracts with continued Vi. The impact of fiber tract orientation will be critical in planning convective delivery for clinical trials, including predictive modeling algorithms for cannula placement and infusate perfusion of anatomical regions.[20,28,30,31]

Prior Cannula Tracts—Cannula tracts from infusions performed previously in the same patient can critically impact infusate distribution. During the second infusion in Case 3 (Table 1), infusate distribution preferentially flowed into a prior cannula tract (previous infusion 4 weeks prior) once the leading edge of infusion encountered this prior tract. This resulted in diversion of the infusate into the previous tract (Fig. 3). Advancing the infusion cannula deeper into the tumor and away from the previous tract mitigated the diversion of the infusate into the prior tract. Consequently, it may be important for the infusion cannula tip to be distant from previous infusion tracts. The period of time needed for infusion tracts to close and the effect of disease state on these tracts are unknown.

Infusion Rate—The optimal and/or maximal rate of convective infusion in the human setting is unknown. Real-time imaging provides direct insight into this critical delivery parameter. The infusions in the current study were progressively increased up to 5 or 10 μl/minute. There was no evidence of leak back along the cannula at the highest rate of infusion (5 or 10 μl/minute; Table 1) except in Case 4 at 10 μl/minute. Despite data in naïve primates that indicate transient infusion rates of 15 μl/minute is safe and feasible without leak back,[22] these clinical findings suggest that rates of 10 μl/minute or more in tumor-invaded tissues may be prone to leak back, underscoring the need for real-time imaging feedback to monitor for this phenomenon and to adjust the infusion rate accordingly.

Vd:Vi Ratio—Previous studies examining direct convective infusate distribution in naïve primate brainstems have revealed that the Vd:Vi ratio ranges from approximately 6:1 to 10:1 in this region of tightly compacted fiber tracts.[16,32] Consistent with a previous report of IL13-PE infusion in a child with a DIPG,[18] the Vd:Vi ratio in our patients was significantly lower (range 1.6–4.1). Notwithstanding the reduction in Vd:Vi ratio due to coinfusion with a lower concentration of Gd-DTPA (Case 1; Gd-DTPA infusion concentration of 1 mM), the reduced efficiency in distribution in these case is likely the result of expansion of the extracellular space due to vasogenic edema.[18,34]

Future clinical trials in disease states associated with vasogenic edema and/or variable cellular density will need to take into consideration the effect of vasogenic edema and/or cellular density on convective Vd. Specifically, it may be possible to use defined MRI

sequences to better determine the size of the interstitial space under a variety of pathological conditions before infusion. This information could, in turn, be used to estimate the efficiency of delivery (that is, Vd:Vi ratio) and the effect of vasogenic edema and/or cellular density in the desired region of infusion. This noninvasive imaging information would have an important effect on treatment planning and trial design.

Accuracy of Gd-DTPA Tracer—In real-time MRI, accurately determining drug Vd is based on the surrogate tracer (that is, Gd-DTPA) moving with the drug through the interstitial spaces similarly. Previous studies have demonstrated that Gd-DTPA (at a 5-mM concentration) accurately tracks a large size range of molecules, including molecules similar in size to IL13-PE.[1,9,15] While it is possible that binding or metabolism of the putative therapeutic agents during infusion could result in a tracer-drug mismatch, we have not observed this with the therapeutic agents we have tested. Because high concentrations of a drug can be homogeneously distributed to CNS tissues by CED, drug binding or metabolic breakdown does not impact distribution compared with inert tracers (for example, Gd-DTPA). Nevertheless, drug-specific features and duration of infusion can potentially have an impact when assessing surrogate imaging accuracy.[5]

Future Implications

Coinfusion of a surrogate-imaging tracer provides critical insight into the clinical effectiveness of drug delivery and a better understanding of the properties of convective delivery. Real-time imaging of coinfused surrogate tracers is feasible and safe. Furthermore, imaging of an infusate provides direct feedback about the effectiveness of drug delivery in various disease conditions and in individual patients. The future application of surrogate imaging will be critical to the clinical application, safety, and effective use of direct convective delivery.

Conclusions

Magnetic resonance imaging of a coinfused Gd-DTPA surrogate tracer provides direct insight into the properties of CED in a clinical application. While clinically relevant Vds can be achieved by convective delivery, specific tissue properties can affect distribution volume and pattern, including Gd-DTPA concentration, preferential flow patterns, and infusion rate. Understanding of these properties of CED can enhance its clinical application.

Acknowledgments

This work was support by the intramural program of the NINDS at the NIH. The IL13-PE was provided by InSys Therapeutics, Inc., under a cooperative research and development agreement with NINDS. The SmartFlow cannula and ClearPoint system were provided by MRI Interventions Inc., under a clinical trial agreement with NINDS.

Abbreviations used in this paper

CED	convection-enhanced delivery
DIPG	diffuse intrinsic pontine glioma
IL13-PE	interleukin-13–*Pseudomonas* exotoxin

ROI	region of interest
Vd	volume of distribution
Vi	volume of infusion

References

1. Asthagiri AR, Walbridge S, Heiss JD, Lonser RR. Effect of concentration on the accuracy of convective imaging distribution of a gadolinium-based surrogate tracer. Laboratory investigation. J Neurosurg. 2011; 115:467–473. [PubMed: 21619409]
2. Bobo RH, Laske DW, Akbasak A, Morrison PF, Dedrick RL, Oldfield EH. Convection-enhanced delivery of macromolecules in the brain. Proc Natl Acad Sci U S A. 1994; 91:2076–2080. [PubMed: 8134351]
3. Bruce JN, Falavigna A, Johnson JP, Hall JS, Birch BD, Yoon JT, et al. Intracerebral clysis in a rat glioma model. Neurosurgery. 2000; 46:683–691. [PubMed: 10719865]
4. Chen MY, Lonser RR, Morrison PF, Governale LS, Oldfield EH. Variables affecting convection-enhanced delivery to the striatum: a systematic examination of rate of infusion, cannula size, infusate concentration, and tissue–cannula sealing time. J Neurosurg. 1999; 90:315–320. [PubMed: 9950503]
5. Croteau D, Walbridge S, Morrison PF, Butman JA, Vortmeyer AO, Johnson D, et al. Real-time in vivo imaging of the convective distribution of a low-molecular-weight tracer. J Neurosurg. 2005; 102:90–97. [PubMed: 15658101]
6. Dickinson PJ, LeCouteur RA, Higgins RJ, Bringas JR, Larson RF, Yamashita Y, et al. Canine spontaneous glioma: a translational model system for convection-enhanced delivery. Neuro Oncol. 2010; 12:928–940. [PubMed: 20488958]
7. Ding D, Kanaly CW, Bigner DD, Cummings TJ, Herndon JE II, Pastan I, et al. Convection-enhanced delivery of free gadolinium with the recombinant immunotoxin MR1-1. J Neurooncol. 2010; 98:1–7. (Erratum in J Neurooncol 98:9, 2010). [PubMed: 19898744]
8. Gimenez F, Krauze MT, Valles F, Hadaczek P, Bringas J, Sharma N, et al. Image-guided convection-enhanced delivery of GDNF protein into monkey putamen. Neuroimage. 2011; 54 (Suppl 1):S189–S195. [PubMed: 20080195]
9. Heiss JD, Walbridge S, Asthagiri AR, Lonser RR. Image-guided convection-enhanced delivery of muscimol to the primate brain. Laboratory investigation. J Neurosurg. 2010; 112:790– 795. [PubMed: 19715424]
10. Jagannathan J, Walbridge S, Butman JA, Oldfield EH, Lonser RR. Effect of ependymal and pial surfaces on convection-enhanced delivery. Laboratory investigation. J Neurosurg. 2008; 109:547–552. [PubMed: 18759589]
11. Krauze MT, Forsayeth J, Yin D, Bankiewicz KS. Convection-enhanced delivery of liposomes to primate brain. Methods Enzymol. 2009; 465:349–362. [PubMed: 19913176]
12. Kunwar S, Chang S, Westphal M, Vogelbaum M, Sampson J, Barnett G, et al. Phase III randomized trial of CED of IL13-PE38QQR vs Gliadel wafers for recurrent glioblastoma. Neuro Oncol. 2010; 12:871–881. [PubMed: 20511192]
13. Laske DW, Youle RJ, Oldfield EH. Tumor regression with regional distribution of the targeted toxin TF-CRM107 in patients with malignant brain tumors. Nat Med. 1997; 3:1362–1368. [PubMed: 9396606]
14. Lonser RR, Gogate N, Morrison PF, Wood JD, Oldfield EH. Direct convective delivery of macromolecules to the spinal cord. J Neurosurg. 1998; 89:616–622. [PubMed: 9761056]
15. Lonser RR, Schiffman R, Robison RA, Butman JA, Quezado Z, Walker ML, et al. Image-guided, direct convective delivery of glucocerebrosidase for neuronopathic Gaucher disease. Neurology. 2007; 68:254–261. [PubMed: 17065591]
16. Lonser RR, Walbridge S, Garmestani K, Butman JA, Walters HA, Vortmeyer AO, et al. Successful and safe perfusion of the primate brainstem: in vivo magnetic resonance imaging of

macromolecular distribution during infusion. J Neurosurg. 2002; 97:905–913. [PubMed: 12405380]

17. Lonser RR, Walbridge S, Murray GJ, Aizenberg MR, Vortmeyer AO, Aerts JM, et al. Convection perfusion of glucocerebrosidase for neuronopathic Gaucher's disease. Ann Neurol. 2005; 57:542–548. [PubMed: 15786474]
18. Lonser RR, Warren KE, Butman JA, Quezado Z, Robison RA, Walbridge S, et al. Real-time image-guided direct convective perfusion of intrinsic brainstem lesions. Technical note. J Neurosurg. 2007; 107:190–197. [PubMed: 17639894]
19. Lonser RR, Weil RJ, Morrison PF, Governale LS, Oldfield EH. Direct convective delivery of macromolecules to peripheral nerves. J Neurosurg. 1998; 89:610–615. [PubMed: 9761055]
20. Morrison, PF. Distribution models of drug kinetics. In: Atkinson, AJ., Jr; Daniels, CE.; Dedrick, RL., et al., editors. Principles of Clinical Pharmacology. New York: Academic Press; 2001. p. 93-112.
21. Morrison PF, Lonser RR, Oldfield EH. Convective delivery of glial cell line-derived neurotrophic factor in the human putamen. J Neurosurg. 2007; 107:74–83. [PubMed: 17639877]
22. Nduom EK, Walbridge S, Lonser RR. Comparison of pulsed versus continuous convective flow for central nervous system tissue perfusion. Laboratory investigation. J Neurosurg. 2012; 117:1150–1154. [PubMed: 23061389]
23. Richardson RM, Kells AP, Martin AJ, Larson PS, Starr PA, Piferi PG, et al. Novel platform for MRI-guided convection-enhanced delivery of therapeutics: preclinical validation in nonhuman primate brain. Stereotact Funct Neurosurg. 2011; 89:141–151. [PubMed: 21494065]
24. Rosset A, Spadola L, Ratib O. OsiriX: an open-source software for navigating in multidimensional DICOM images. J Digit Imaging. 2004; 17:205–216. [PubMed: 15534753]
25. Sampson JH, Archer G, Pedain C, Wembacher-Schröder E, Westphal M, Kunwar S, et al. Poor drug distribution as a possible explanation for the results of the PRECISE trial. Clinical article. J Neurosurg. 2010; 113:301–309. [PubMed: 20020841]
26. Sampson JH, Brady M, Raghavan R, Mehta AI, Friedman AH, Reardon DA, et al. Colocalization of gadolinium-diethylene triamine pentaacetic acid with high-molecular-weight molecules after intracerebral convection-enhanced delivery in humans. Neurosurgery. 2011; 69:668–676. [PubMed: 21430586]
27. Sampson JH, Brady ML, Petry NA, Croteau D, Friedman AH, Friedman HS, et al. Intracerebral infusate distribution by convection-enhanced delivery in humans with malignant gliomas: descriptive effects of target anatomy and catheter positioning. Neurosurgery. 2007; 60(2 Suppl 1):ONS89–ONS99. [PubMed: 17297371]
28. Sampson JH, Raghavan R, Brady ML, Provenzale JM, Herndon JE II, Croteau D, et al. Clinical utility of a patient-specific algorithm for simulating intracerebral drug infusions. Neuro Oncol. 2007; 9:343–353. [PubMed: 17435179]
29. San Sebastian W, Richardson RM, Kells AP, Lamarre C, Bringas J, Pivirotto P, et al. Safety and tolerability of magnetic resonance imaging-guided convection-enhanced delivery of AAV2-hAADC with a novel delivery platform in nonhuman primate striatum. Hum Gene Ther. 2012; 23:210–217. [PubMed: 22017504]
30. Sarntinoranont M, Banerjee RK, Lonser RR, Morrison PF. A computational model of direct interstitial infusion of macromolecules into the spinal cord. Ann Biomed Eng. 2003; 31:448– 461. [PubMed: 12723686]
31. Sarntinoranont M, Iadarola MJ, Lonser RR, Morrison PF. Direct interstitial infusion of NK1-targeted neurotoxin into the spinal cord: a computational model. Am J Physiol Regul Integr Comp Physiol. 2003; 285:R243–R254. [PubMed: 12793999]
32. Souweidane MM, Occhiogrosso G, Mark EB, Edgar MA. Interstitial infusion of IL13-PE38QQR in the rat brain stem. J Neurooncol. 2004; 67:287–293. [PubMed: 15164984]
33. Souweidane MM, Occhiogrosso G, Mark EB, Edgar MA, Dunkel IJ. Interstitial infusion of carmustine in the rat brain stem with systemic administration of O6-benzylguanine. J Neurooncol. 2004; 67:319–326. [PubMed: 15164987]

34. Wood JD, Lonser RR, Gogate N, Morrison PF, Oldfield EH. Convective delivery of macromolecules into the naive and traumatized spinal cords of rats. J Neurosurg. 1999; 90 (1 Suppl):115–120. [PubMed: 10413135]

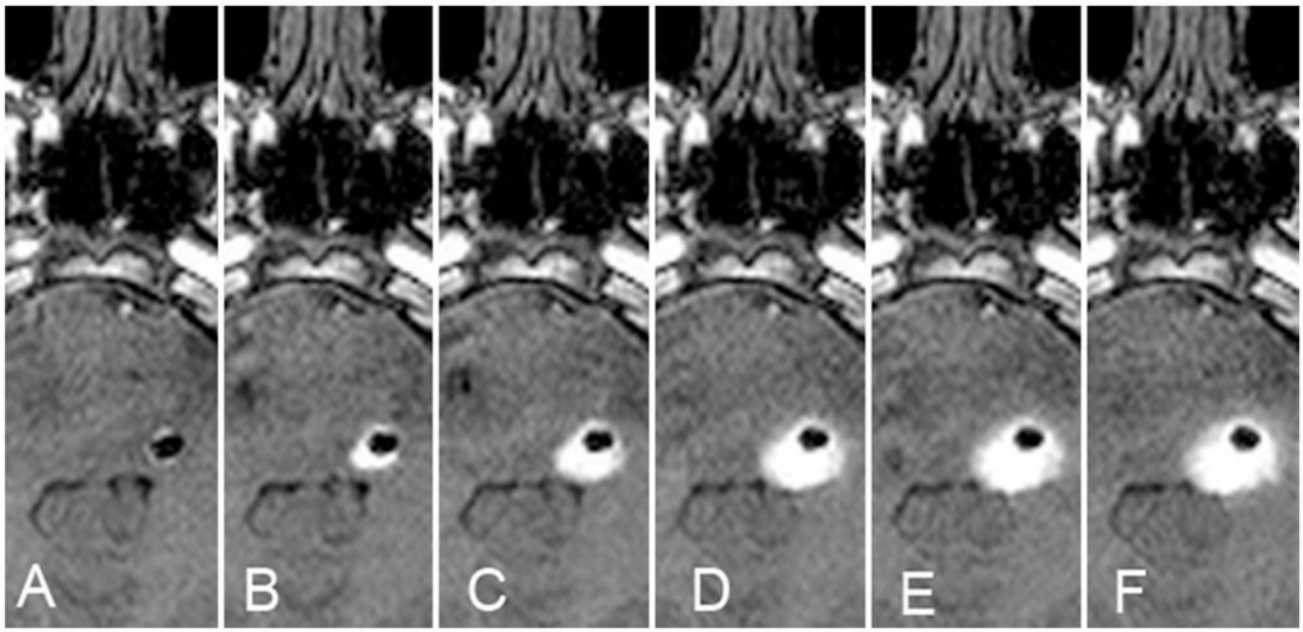

Fig. 1.

Case 1. Intraparenchymal air effects on infusate distribution. **A–F:** Serial axial T1-weighted MR images obtained every 100 minutes, demonstrating the impact of intraparenchymal air (hypointensity) introduced at the start of the infusion after removal of an internal stylet. While there was a small decrease in the volume of air over time, the serial images demonstrate the restriction of anteromedial spread of infusate (hyperintensity) by the air in the parenchyma.

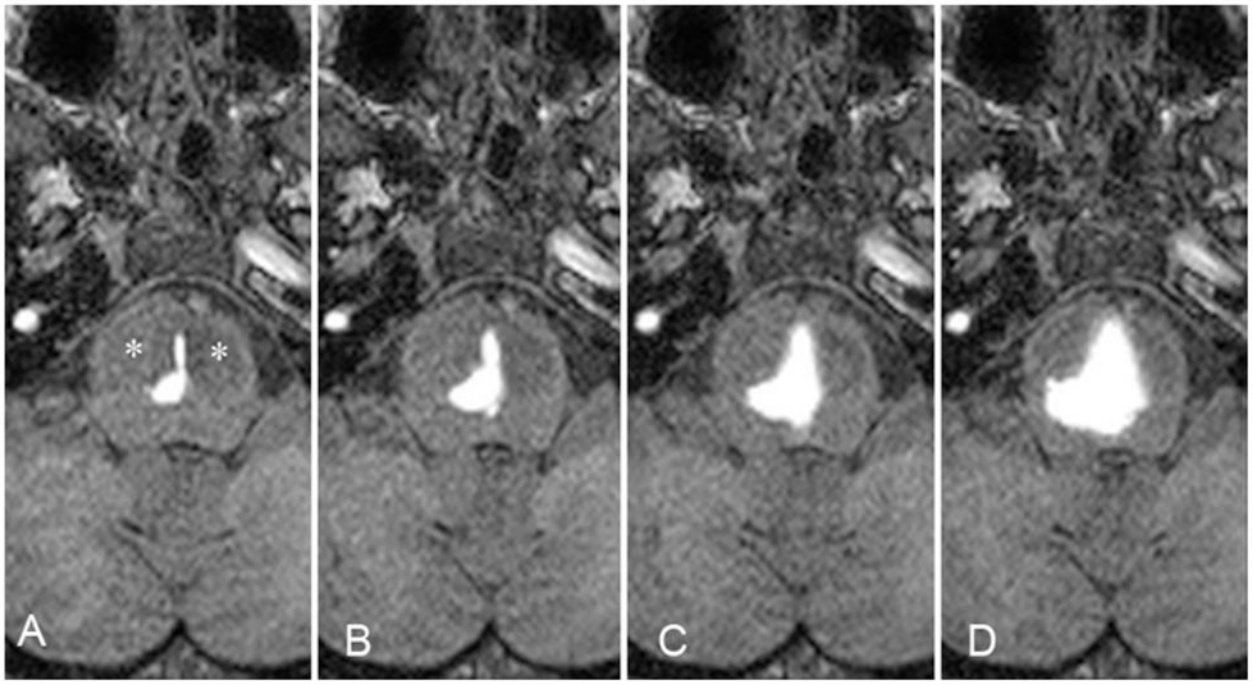

Fig. 2.

Case 3. Preferential infusate flow along parallel white matter tracts. **A–D:** Serial axial T1-weighted MR images acquired every 50 minutes, demonstrating preferential infusate flow in the white matter tracts of the brainstem in the axial plane. The serial images demonstrate preferential spread of infusate along the horizontal fibers of the pons that initially preserve the perpendicularly oriented corticospinal tracts.

Fig. 3.

Case 3. Preferential infusate flow into a previous infusion cannula tract. The previous infusion cannula tract is visualized *(white arrows)* on sagittal T1-weighted MR image. Once the leading edge of the second infusion *(black arrows)* encounters the previous cannula tract, the infusate preferentially flows into the prior tract *(arrowheads)*.

Fig. 4.

Case 4. Infusate leak back along the cannula at highest rate of infusion. Sagittal T1-weighted MR image demonstrating infusate leak back *(arrowheads)* along the cannula at 10 μl/minute.

TABLE 1

Infusion characteristics in patients

Case No.	Age (yrs), Sex	Gd-DTPA (mM)	IL13-PE (μg/ml)	Infusion Device	Final Infusion Rate	Total Vol Infused (ml)	Final Vd:Vi	Findings
1	10, F	1	0.125	catheter	5	2.8	1.6	reduced imaging Vd consistent w/lower Gd-DTPA concentration; intraparenchymal air directed infusate away from anteromedial tumor
2	16, M	5	0.125	cannula	5	2.3	4.1	continuous perfusion w/o interruption
3	17, M	5	0.125	cannula	10	3.7	4.0	at 95 mins, infusate leaked at inline filter connection; connection replaced & perfusion continued w/o incident
		5	0.125	cannula	10	3.0	3.4	preferential flow of infusate into prior cannula track (from 1st infusion 4 wks earlier)
4	5, F	5	0.25	cannula	10	1.1	1.9	leak back along cannula track at highest rate of infusion (10 μl/min)